

# Calculation of detection limits for a single-laboratory ion-chromatographic method to determine parts-per-trillion ions in ultrapure water

L.E. Vanatta<sup>a,\*</sup>, D.E. Coleman<sup>b</sup>

<sup>a</sup>Texas Instruments, Box 650311, MIS 301, Dallas, TX 75265, USA

<sup>b</sup>Alcoa Technical Center, AMCT-D-10, 100 Technical Drive, Alcoa Center, PA 15069, USA

## Abstract

This paper addresses the calculation of detection limits (DLs) for ion-chromatographic data at low parts-per-trillion (w/w) levels. The main objectives are: (1) to explain two statistical techniques (the EPA or “ $3\sigma$ ” approach and the Hubaux–Vos method), (2) to calculate DLs using each procedure, (3) to discuss the strengths and weaknesses of each statistical approach and (4) to decide if the analytical method is appropriate for quantifying anions at the 50-ppt level in deionized water. The analytes of interest are: fluoride, chloride, nitrite, bromide, nitrate, sulfate and phosphate. All work was performed on a Dionex DX500 microbore unit, using an AS11 column. Results indicate that the H–V method gives a more realistic (and higher) DL than does the  $3\sigma$ . Assuming false-negative and false-positives probabilities of 10% or less, this analytical method is not acceptable for quantifying anions at the desired level.

**Keywords:** Detection limit; Water analysis; Anions

## 1. Introduction

In the manufacture of semiconductors, the demand is growing for ultrapure water with anion specifications in the low parts-per-trillion (ppt) (w/w) [1]. Consequently, the need exists for analyzing grab samples, using laboratory methods with known detection limits (DLs). A DL is defined to be the concentration below which the analytical method cannot reliably detect a response [2]. Ion chromatography can be used for these tests by using concentrator columns instead of injection loops, and by observing contamination-control procedures [3]. Calibration curves are generated with the instrumental software and detection limits are calculated by some method. A widely utilized DL technique is

known commonly as the  $3\sigma$  approach, which is mandated for EPA testing [2]. This calculation is easy to make, but the result takes into account only the data for blanks; it does not consider calibration curves. In contrast, the Hubaux–Vos (H–V) procedure [4] respects blanks, calibration and standards; this method is more statistically sound.

The theory behind the H–V technique is discussed in various references [5–8]. Several researchers have reported results using the H–V formula [9–11], but none has applied it to low-level ion-chromatographic analyses. The purpose of this paper is to investigate the use of the  $3\sigma$  and H–V procedures with such data, and to compare the results.

Anion standards in the 50-ppt range and blanks were analyzed with a Dionex AS11 microbore gradient separation. Using the  $3\sigma$  method, DLs were calculated from these data. For the H–V approach,

\*Corresponding author.

calibration curves were generated using ordinary least squares (OLS) for blanks and eight levels of standards, which ranged from 25 to 200 ppt. Next, the calibration curve for each anion was evaluated statistically to determine if an acceptable model had been used. Finally, detection limits were calculated.

## 2. Experimental

### 2.1. Materials

Sodium hydroxide, 50% w/w with  $\leq 0.10\%$  sodium carbonate, from Fisher Scientific (Pittsburgh, PA, USA) was used to prepare eluent solutions of 200 mM and 5 mM NaOH. Working-standard solutions of fluoride, chloride, bromide, nitrate, sulfate and phosphate were prepared from 1000-ppm (w/w) stock standard solutions from National Institute of Standards and Technology (Gaithersburg, MD, USA); those of nitrite were made from 1000-ppm standards from Alltech Associates (Deerfield, IL, USA). Deionized water (18 m $\Omega$  cm) was provided by a point-of-use water purification system (Ahlfinger Water, Dallas, TX, USA).

Water for eluents was sparged with helium before solutions were mixed. The mobile phases then were kept under pressure with helium throughout their life. Working standards ranged in concentration from 25 to 200 ppt.

### 2.2. Apparatus and columns

A Dionex (Sunnyvale, CA, USA) DX500 micro-bore ion chromatograph was utilized for all work. Unless otherwise noted, all instrument modules and consumables were from Dionex Corp. Analytical columns used were an IonPac AG11 Guard (2 mm $\times$  50 mm) with AS11 Analytical (2 mm $\times$  250 mm). A GP40 Gradient Pump delivered the eluent at a flow of 0.5 ml/min; the gradient program is given in Table 1. Post-column eluent suppression was accomplished with an Anion Self-Regenerating Suppressor (ASRS-I, 2 mm) in the external-water mode; detection was via a CD20 Conductivity Detector at an output range of 10  $\mu$ S. For preconcentrating samples, a TAC-LP1 (4 mm $\times$  35 mm) concentrator column was used. To load the TAC-LP1, high-purity helium

Table 1  
Gradient program for AS11 column

Time (min)	%1	%2	%3
0.0	90	10	0
0.2	90	10	0
2.5	90	10	0
6.0	0	100	0
18.0	0	83	17

Eluent 1: Deionized water.

Eluent 2: 5 mM NaOH.

Eluent 3: 200 mM NaOH.

Flow rate = 0.5 ml/min.

pressurized the sample bottle in a modified Dionex reagent-delivery module [3]. The column was loaded at a flow rate of 0.75 ml/min with a pressure of 586 kPa (85 p.s.i.) for 16 min to deliver a volume of  $12.0 \pm 0.05$  ml of sample. All tubing in the chromatography path (from the outlet of the pump to the exit of the suppressor) was PEEK [0.005 in (0.125 mm) I.D.]. Instrument control and data collection were performed with a personal computer and Dionex PeakNet software. Statistical calculations were carried out using JMP software (SAS Institute, Cary, NC, USA).

### 2.3. Standards preparation

A stock standard containing 5 ppm (w/w) of each anion was prepared from the commercial solutions and used throughout the investigation. This standard was made by diluting 1 g of each NIST solution to 200 g. An XT Top Loading Balance (Fisher Scientific) was used for the one weighing of 200 g; the weight was recorded to two decimal places. All other weighings (each to four decimal places) were made on a Sartorius MC1 Analytical Balance. The concentration of each solution was calculated from these readings. Each week, a 50-ppb (w/w) standard was prepared from the stock by diluting 1 g to 100 g. On a daily basis, 1.5 g of the 50 ppb was diluted out to 150 g to give a 500-ppt solution. For all working standards (25, 37.5, 50, 62.5, 75, 100, 150 and 200 ppt), the appropriate weight of the 500-ppt standard was diluted to 100 g. (This concentration range was chosen because of contamination specifications of ultrapure-water users [1].)

Dilution errors in the daily working standards were estimated by conducting a Monte Carlo simulation. This exercise was based on the upper bounds on the magnitude of weighing error for the scales (0.01 g for the XT Balance and 0.0001 g for the Analytical Balance). In the simulation, weighing errors were randomly drawn from a Normal distribution with mean equal to zero and standard deviation equal to the upper bound. The distribution of these relative concentration errors was found never to exceed 0.1% relative error, which was considered negligible.

Polystyrene tissue-culture flasks with plug seals (Corning, Corning, NY, USA) were used for all preparations. Polyethylene transfer pipettes (Fisher Scientific) were used to deliver 1000-ppm standards. For all subsequent dilutions, transfers of standards were done by pouring, since pipettes contaminated at these levels.

At the end of each day, the flasks were emptied, rinsed thoroughly, and then filled with deionized water. The same flask was used for the same standard each time. System blanks were prepared in a separate flask, using the same procedure as that used for making the working standards, except that deionized water was added instead of 500-ppb standard. All eight standards and one system blank were prepared and analyzed (in random order) on eight separate days. The first four days, one 50-ppb standard was used for dilutions, while a second such solution was utilized on the other four days.

### 3. Results and discussion

A typical chromatogram for a 50-ppb standard is shown in Fig. 1a; the corresponding system blank is given in Fig. 1b. All ions of interest eluted in under 15 min. Along with the seven analytes, several contaminant peaks were detected as well. These are identified where possible.

In the following sections, three terms are used and are defined as follows:

1. Run: any series of standards prepared and analyzed all on one day. The Run numbers are given chronologically. In this experiment, there was a total of eight Runs.
2. Level: the concentration of a standard (includes blanks).

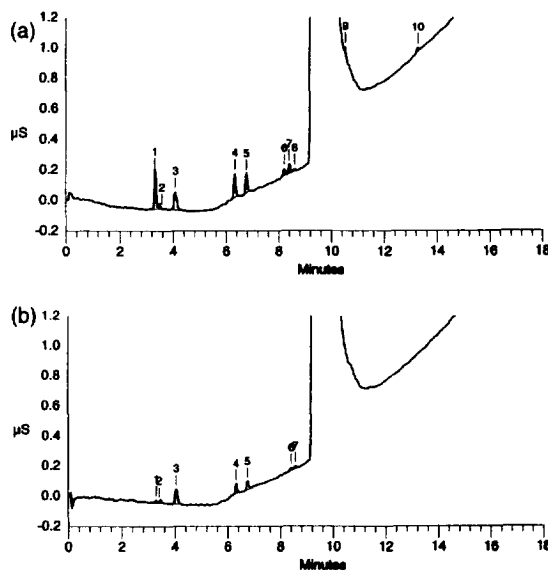


Fig. 1. (a) A chromatogram of a 12-ml aliquot of a seven-anion standard (50 ppt each) in deionized water. Peak identities: 1 = fluoride; 2 = acetate (contaminant); 3 = formate (contaminant); 4 = chloride; 5 = nitrite; 6 = bromide; 7 = nitrate; 8 = unknown contaminant; 9 = sulfate; 10 = phosphate. (b) A chromatogram of the accompanying system blank. Peak identities: 1 = fluoride; 2 = acetate (contaminant); 3 = formate (contaminant); 4 = chloride; 5 = nitrite; 6 = nitrate; 7 = unknown contaminant. Experimental conditions for both tracings are those given in Table 1 and in Section 2.

3. Sequence: any set of Runs made in chronological order. For example, a Sequence of four would be Runs from days 1, 2, 3 and 4; or from days 5, 6, 7 and 8.

All mathematical symbols used in this section are defined in the Appendix at the end of the paper.

#### 3.1. Detection-limit theory

Two methods were examined for calculating detection limits. The first is known as  $3\sigma$  [2] and the second as Hubaux-Vos [4]. Both methods involve the concept of a frequency distribution that results when a blank is analyzed in replicate. If measurement response is plotted on the  $x$ -axis and frequency of occurrence on the  $y$ -axis, a Normal (i.e., Gaussian) "bell-shaped" curve usually results. Associated with the instrument or method is a threshold ( $T$ ), which is the response that is the cut-off between detection and non-detection. This threshold will

intersect the blank's frequency curve at some point on its right tail. The area under the Normal curve to the right of the cut-off is known as  $\alpha$ , and is the probability of false positives.  $\alpha$  and  $T$  are linked; once one is defined, the other is implicitly set (see Fig. 2).

The  $3\sigma$  approach calculates a DL based on the blanks or a trace-level standard alone. Often, three times the standard deviation of the blank measurements is chosen [2]. The result is a DL that has a defined value of  $\alpha$ . Ignored are the concept of false negatives, calibration curves, bias (true minus reported value), and any non-constant variation as concentration changes.

In contrast, H-V also considers the variance when a low-level standard is tested. The threshold will intersect the resulting frequency distribution, this time in the left-hand tail (see Fig. 2). Any measurement to the left of (i.e., below) the threshold will not be detected; thus, the area of the left tail is the probability of false negatives and is known as  $\beta$ . The concepts of  $\alpha$  and  $\beta$  are both illustrated in Fig. 2.

Hubaux-Vos also uses the calibration curve that is generated by analyzing low-level standards that bracket the range of interest. From statistical calculations, upper and lower prediction limits can be derived and plotted along with the curve (see Fig. 3). If the plot is expanded to three dimensions, the frequency distributions can be graphed in the  $y$ - $z$  plane. For convenience in Fig. 3, curves in this plane have been projected onto the  $x$ - $y$  grid. The upper prediction limit intersects the  $y$ -axis at the threshold; thus, the proportion  $\alpha$  of all the blank measurements

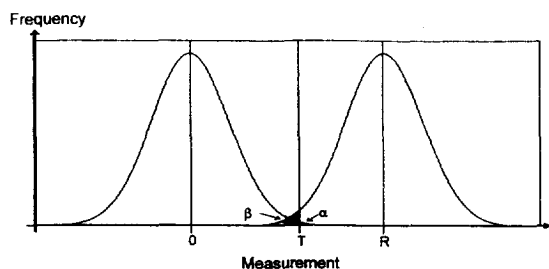


Fig. 2. Plot showing intersection of frequency curves for a blank (Response=0) and for a low-level standard (Response= $R$ ) with the threshold,  $T$ . The probability of false positives ( $\alpha$ ) is the blank graph's area to the right of  $T$ ; the probability of false negatives ( $\beta$ ) is the standard curve's area to the left of  $T$ .

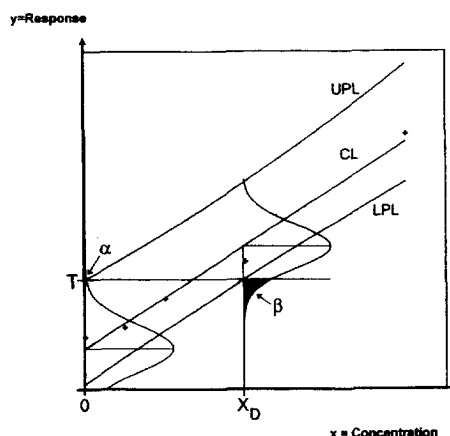


Fig. 3. Graphical depiction of the Hubaux-Vos method of calculating detection limits. The concentration,  $x_D$ , is the detection limit. UPL=upper prediction limit; CL=calibration line; LPL=lower prediction limit. See text for details.

will be above this limit and will be detected falsely. The lower limit is such that the proportion  $\beta$  of all measurements of samples at any given concentration will fall below the limit.

A line drawn through  $T$  and parallel to the  $x$ -axis will intersect the lower limit at some concentration,  $x_D$ . With probability  $\beta$ , the measured response will fall below  $T$  and therefore will not be detected. Thus, at  $x_D$ ,  $\beta$  is the probability of false negatives and  $\alpha$  is the probability of false positives. This concentration is the H-V detection limit. It is the minimum true concentration that can be measured reliably, with the probability of false negatives held at  $\beta$ . This DL, then, captures: (1)  $\alpha$  and  $\beta$ , (2) calibration, (3) bias and (4) non-constant  $\sigma$ . (If measurement standard deviation varies with concentration, then weighted least squares (WLS) should be used instead of OLS to generate the calibration line, prediction limits and DL.)

This study used the advisable practice of first choosing values of  $\alpha$  and  $\beta$  were chosen first. Then the calibration curve and prediction limits were calculated using the statistical software. A plot similar to the above was generated. Finally, the two lines were drawn and the detection limit was calculated from the  $x$ -axis.

A more accurate value for the H-V DL can be obtained from a recursive formula:

$$x_{D} = s/b\{[t_{1-\alpha, n-2} \cdot R(0)] + [t_{1-\beta, n-2} \cdot R(x_{D_{est}})]\}, \quad (1)$$

where  $R(z) = \{1 + 1/n + [(z - x_{avg})^2 / S_{xx}]\}^{1/2}$ ,

$s$  = sample standard deviation (often, RMSE is used),

RMSE = root mean square error,

$b$  = slope of the calibration line,

$t$  = Student's  $t$ ,

$n$  = number of measurements in the calibration design,

$x_{D_{est}}$  = an estimate of the DL,

$z$  = a concentration,

$x_{avg}$  = average of the concentrations in the calibration design,

$S_{xx}$  = the sum of all  $(x - x_{avg})^2$ .

With this formula, an initial estimate was made for  $x_{D_{est}}$  (in most cases,  $5s/b$  is used). A new value of  $x_{D_{est}}$  was calculated and then iterations took place as many times (usually two or three) as needed.

### 3.2. Calculation of DL using the $3\sigma$ method

The  $3\sigma$  DL is easy to calculate and thus is used often (and sometimes is mandated) [2]. Two approaches are allowed. The faster is simply to compute the standard deviation of blank replicates ( $\geq 7$ ) and divide by the slope of the calibration curve. The result is the standard deviation in concentration units. This number then is multiplied by the appropriate value of Student's  $t$  (i.e., for the chosen  $\alpha$  and for  $n - 1$  degrees of freedom), resulting in the detection limit. Student's  $t$  is roughly three for the often-used

$\alpha$  of 0.01 and for seven or eight replicates, thereby giving this calculation its name [2].

The second calculation involves analyzing replicates (again, seven or more) of a low-level standard and making the above calculation. If the estimated DL is greater than one-fifth the value of the concentration used, then the number can be used as the detection limit.

This protocol, then, does not involve the use of calibration curves, except to provide a slope value to convert the response's standard deviation to concentration units. It relies solely on the analysis of replicates of blanks or low-level standards.

The technique was applied to three different Levels of all seven ions, using all eight Runs in each case.  $\alpha$  was chosen to be 0.01. The Levels involved were the blank, the 25 ppt and the 37.5 ppt. (One value for bromide was eliminated in the 37.5 level, since that number was determined to be an outlier.) Results are shown in Table 2. Most anions gave a wide range of values. Consequently, this technique is not very precise. Even more important, the method addresses only the issue of false positives, keeping them at 1% if  $\alpha = 0.01$ . The probability of false negatives (when measuring at the DL concentration) is not incorporated, is unknown and uncontrolled. Consider the case when the  $3\sigma$  DL is used as the threshold. When a sample with a true concentration equal to this DL is analyzed, its frequency distribution will be centered at the threshold,  $T$ . Since  $T$  is the cut-off between "detect" and "non-detect", half of the plot will fall to the left of  $T$  and thus will not be seen. Hence, approximately 50% of the time, the detection decision will be incorrect!

Table 2  
Detection limits ( $3\sigma$ ) for each anion

Ion	DL from Blank	DL from 25 ppt	DL from 37.5 ppt
Fluoride	7.2	12.8	11.8
Chloride	9.2	15.8	13.9
Nitrite	49.3	44.6	39.3
Bromide	NA	17.5	8.6
Nitrate	22.6	34.0	46.4
Sulfate	NA	NA	54.0
Phosphate	NA	33.8	27.2

DLs (all in ppt) are calculated using the various  $3\sigma$  approaches ( $\alpha = 0.01$ ). For blanks, the result is the detection limit. For low-level standards, the value must be greater than one-fifth the concentration itself; if this test is passed, the number may be used for the DL. In these cases, all computations are valid DLs. (Note: NA = not applicable; in these instances, no integratable response was obtained.)

### 3.3. Calculation of DL via Hubaux–Vos method

#### 3.3.1. Evaluation of calibration curves

Calibration curves (using the technique of OLS) were generated for each anion, using all eight Runs and all nine Levels (again, one 37.5-ppt result for bromide was an outlier and was eliminated from all calculations). Before any DLs were calculated, each graph was analyzed statistically to see if the chosen model was appropriate. Two tests were applied: (1) a “significance test” for the slope of the calibration line and (2) a lack-of-fit test.

The first involves the calculation of a term,  $g$ :

$$g = [(\text{RMSE})^2 \cdot (t_{n-2, 1-\alpha/2})^2] \div [(b^2) \cdot (S_{xx})]. \quad (2)$$

The result should be less than 0.1 for each curve; all calibrations met this criterion.

The second test is crucial, since it indicates whether an appropriate model has been used. One way to assess the fit is to examine the residuals, which should be random about zero. If the pattern flares out as concentration increases (i.e., if there is non-constant response variation), then WLS should be used instead. If the residuals do not vary about zero, then a straight line may not be applicable, or the range of concentrations may be too high.

A more exact determination of the lack of straight-line fit can be made by looking at the  $p$ -value for the lack-of-fit test; this value is labelled “Prob>F” in the “Lack of Fit” portion of the “Fit Model” choice in JMP. This value should be greater than 0.01 at minimum, and preferably greater than 0.05.

In this experiment, no residual pattern indicated the need for WLS. All curves but bromide and phosphate had lack-of-fit results above 0.01. However, sulfate and fluoride were both at only 0.027. Deleting the 150- and 200-ppt Levels brought the fluoride curve to 0.08, thus indicating that some non-linearity existed above 100 ppt. As a result, this new curve was the one used for calculations. The sulfate value did not change when the range was restricted. However, the chromatographic response for that anion, and for phosphate as well, was determined to be too weak and too variable to yield an appropriate calibration curve. Thus, the best

action in these two cases probably is to improve the separation before performing a DL calculation. Consequently, these two analytes were dropped from further computations. The lack-of-fit test for bromide was found to be above 0.05 only in the restricted range of 25 to 75 ppt. Hence, that calibration curve was the one used. However, any report for bromide should note that no blank was included in the calculation.

Thus, for all anions except sulfate and phosphate, the calibration-curve model was a straight line, with normally distributed measurement errors, having homogeneous variance. Therefore, OLS could be applied to data as described above.

Two other parameters were examined: (1)  $R_{\text{adj}}^2$ , which has an ideal value of 1 and (2)  $\text{RMSE}/b$ , which is the standard deviation of the measurement error in concentration units (i.e., a measure of precision). With both terms, it is up to the user to determine whether the values for these two parameters are acceptable. While only chloride’s  $R_{\text{adj}}^2$  was above the usually desired value of 0.99, all other values were for curves that came from acceptable models. It should be noted that having a high  $R_{\text{adj}}^2$  does not necessarily indicate linearity [12]. For example, the OLS curve for nine-Level, eight-Run fluoride had an  $R_{\text{adj}}^2$  of 0.994, but tests showed that model to be inappropriate.

#### 3.3.2. Hubaux–Vos calculations

If OLS is an applicable fitting method, the H–V DL can be approximated from a graph obtained using JMP. Via the “Fit  $Y$  by  $X$ ” routine, the calibration curve is plotted by choosing “Fit Line” under “Fitting”. The prediction limits are added by selecting “Confid Curves: Indiv” under “Linear Fit”; these lines are for  $\alpha = \beta = 0.025$ . The lower portion of the graph is enlarged and printed out. To determine the DL, the appropriate lines are drawn, as described above in Section 3.1. An example is shown in Fig. 4, which is for chloride’s nine-Level, eight-Run curve. The approximate DL is 21 ppt.

The recursive formula was used to calculate accurate values for fluoride, chloride, nitrite, bromide and nitrate, using the calibration curves that were appropriate in each case. Results are given in Table 3 ( $\alpha = \beta = 0.01$ ); also included are  $R_{\text{adj}}^2$  and  $\text{RMSE}/b$ .

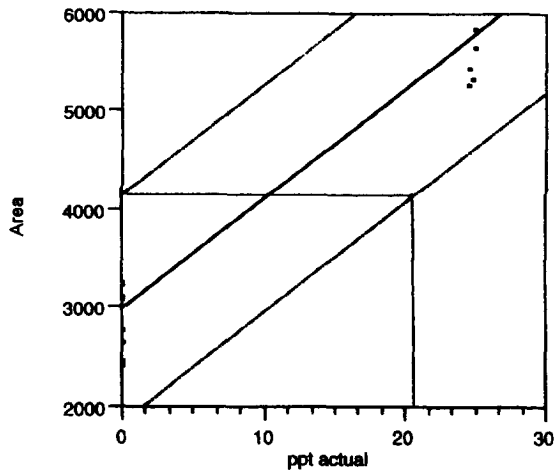


Fig. 4. Graphical determination of the Hubaux-Vos detection limit for chloride ( $\alpha = \beta = 0.025$ ;  $n = 72$ ; OLS calibration curve; range of standards = 0 to 200 ppt, as enumerated in Section 2.3). Note: only the range of 0 to 30 ppt is shown in the figure.

### 3.4. Comparison of $3\sigma$ and Hubaux-Vos DLs

As seen from Table 2, the maximum  $3\sigma$  DLs (in ppt) were: 12.8 for fluoride, 15.8 for chloride, 49.3 for nitrite, 17.5 for bromide and 46.4 for nitrate. In contrast, H-V results ( $\alpha = \beta = 0.01$ ) were 18.0, 24.8, 80.0, 21.9 and 54.2 ppt, respectively. These data show that the  $3\sigma$  DLs were too low in all cases. H-V DLs are higher and more useful because they respect not only the probability of false positives ( $\alpha$ ), but also the probability of false negatives ( $\beta$ ) and the calibration process.

### 3.5. Effect of calibration design on H-V detection limits

To study the effect of calibration design on the H-V DL, data from chloride and nitrite analyses

Table 3  
Hubaux-Vos detection limits for  $\alpha = \beta = 0.01$

Ion	H-V detection limit	$R^2_{adj}$	RMSE/ $b$
Fluoride	18.0	0.9864	3.670
Chloride	24.8	0.9926	5.136
Nitrite	80.0	0.9302	16.594
Bromide	21.9	0.9490	4.172
Nitrate	54.2	0.9659	11.243

See text for discussion of calibration curves used. All DLs in ppt.

Table 4  
Effect of calibration design on H-V detection limit for chloride ( $\alpha = \beta = 0.01$ )

Chloride Levels used in each curve (in ppt)									H-V DL (in ppt)
0	25	37.5	50	62.5	75	100	150	200	
X	X	X	X	X	X	X	X	X	24.8
X	X		X		X	X	X	X	24.8
X	X		X			X		X	25.5
X			X			X	X	X	25.9
X	X	X	X	X	X	X			23.2
X	X		X		X	X			22.3
X	X		X			X			23.1
X			X			X			22.2

were chosen. Several reasons led to these selections. Both anions demonstrated acceptable OLS curves using all nine Levels and eight Runs. In addition, the two had similar response factors and levels in the blank (see Fig. 1a and Fig. 1b). However, their accompanying DLs were very different: 24.8 ppt for chloride vs. 80.0 ppt for nitrite, assuming  $\alpha = \beta = 0.01$ .

These two, then, were examined to see the effect of calibration design (and later,  $\alpha$  and  $\beta$ , and Sequence size) on the H-V DL. For the design study,  $\alpha$  and  $\beta$  were kept at 0.01, and all eight Runs were used in every case. Data are presented in Table 4 for chloride and in Table 5 for nitrite. No significant difference was determined for chloride, with the DLs ranging from 22.2 to 25.9 ppt. For nitrite, a wider range was seen, running from 75.1 to 88.3 ppt. With both ions, lower values were obtained by restricting the top Level to a concentration of 100 ppt.

Table 5  
Effect of calibration design on H-V detection limit for nitrite ( $\alpha = \beta = 0.01$ )

Nitrite Levels used in each curve (in ppt)									H-V DL (in ppt)
0	25	37.5	50	62.5	75	100	150	200	
X	X	X	X	X	X	X	X	X	80.0
X	X		X		X	X	X	X	83.9
X	X		X			X		X	83.3
X			X			X	X	X	88.3
X	X	X	X	X	X	X			75.1
X	X		X		X	X			80.0
X	X		X			X			79.2
X			X			X			84.8

Table 6  
Effect of  $\alpha$  and  $\beta$  on H–V DLs for chloride and nitrite

Ion	H–V DL for:			
	$\alpha=\beta=0.01$	$\alpha=\beta=0.025$	$\alpha=\beta=0.05$	$\alpha=\beta=0.10$
Chloride	24.8	20.8	17.4	13.5
Nitrite	80.0	67.0	56.1	43.5

For both ions, all nine Levels and all eight Runs were used to generate a calibration curve and then the DL. All DLs in ppt.

### 3.6. Effect of $\alpha$ and $\beta$ on H–V detection limits

This study looked at the effect of changing the value of  $\alpha$  and  $\beta$ . Here, the eight-Run, nine-Level calibration curve was used for both chloride and nitrite. Detection limits for  $\alpha=\beta=0.01$ , 0.025, 0.05 and 0.10 were calculated, and are given in Table 6. Adjusting the  $\alpha$  and  $\beta$  values from 0.10 to 0.01 nearly doubled the DL. These detection limits give a clear indication of the importance of choosing and reporting  $\alpha$  and  $\beta$  when calculating DLs.

### 3.7. Effect of Sequence size on H–V detection limits

In the above discussion, H–V DLs were calculated using chloride and nitrite data from all eight Runs. It would be more convenient and time-saving if a smaller number of Runs were used. Generally, fewer Runs in a calibration study will result in a DL that is slightly higher, because of the higher value of Student's *t* statistic associated with fewer degrees of freedom. This general tendency is easily obscured by the variability in the estimated standard deviation and, hence, in the DL. The other issue is how fewer Runs may affect the variability in the calculated DL

Table 7  
Comparison of H–V DLs for various Sequences

Number of Sequences in each calibration curve	Number of calibration studies used	Average H–V DL for chloride	Chloride R.S.D.	Average H–V DL for nitrite	Nitrite R.S.D.
8	1	24.80	NA	80.00	NA
4	2	25.70±0.71	2.8%	69.60±6.79	9.8%
2	4	25.78±6.49	25.2%	74.40±20.85	28.0%
1	8	27.10±13.24	48.9%	63.15±29.04	46.0%

Nine Levels were used in each Run. In all cases,  $\alpha=\beta=0.01$ . NA=Not applicable. See text for detailed explanation of Sequence construction. All DLs in ppt.

(every calculated DL is an estimate of the true, unknown DL).

To investigate this other issue, nine-Level Sequences were formed, first with four Runs. No Run was reused in forming the groups. Here, two possible Sequences existed: Runs 1 through 4, and Runs 5 through 8. A H–V DL was calculated for each Sequence, using  $\alpha=\beta=0.01$ . Then an average, standard deviation, and R.S.D. were computed for the two values, giving  $25.70\pm0.71$  (2.8%) for chloride and  $69.60\pm6.79$  (9.8%) for nitrite. In like manner, summary statistics were determined for Sequences containing two Runs, and for those with only one Run. Data are presented in Table 7.

These findings indicate that restricting the number of Runs can significantly compromise the precision of the DL. Even though eight values were averaged for the single-Run DLs, the R.S.D. was almost 50% for both anions.

## 4. Conclusions

Although the  $3\sigma$  detection limit was easier to calculate and required only a minimum of data, the results yielded lower values than were realistic. On the other hand, Hubaux–Vos calculations took into account calibration curves and  $\beta$ , as well as  $\alpha$ . In addition, this procedure could accommodate (if necessary) non-constant response variation by using WLS to generate the calibration curve.

In this study,  $\alpha$  and  $\beta$  were each  $\leq 10\%$ . The calculated H–V detection limits were found to be too high to use this analytical method for quantifying anions at the 50-ppt level.



A H–V DL can be calculated for any calibration curve, but that graph should be tested first to be sure an appropriate model has been chosen. As can be seen from the recursive formula in Section 3.1, the DL will depend primarily on two parameters: (1)  $s/b$  and (2) Student's  $t$ . If the degrees of freedom and/or the risk factors of  $\alpha$  and  $\beta$  are low, then a higher DL will result because of a larger value for Student's  $t$ .

If a H–V DL is unacceptably high, it can be reduced by: (1) assuming more risk of false positives or false negatives, (2) increasing the sample size or (3) improving the precision of the analytical method. In any case, it is important to remember that DLs are not simply absolute numbers that stand by themselves; they are a matter of probabilities. Thus, degrees of freedom,  $\alpha$  and  $\beta$  should be stated along with the DL itself. In addition, mention should be made of the calibration design that was used. Such a report will give the analyst a clear and accurate assessment of the usefulness of the DL and the analytical method.

## Acknowledgments

The authors would like to acknowledge: Ruthann Kiser of Dionex Corporation for her helpful suggestions concerning the chromatography; Robert Gibbons, Nancy Grams, Ray Maddalone, Lloyd Currie, Charles Davis, Babu Nott, Jim Rice, Phil Ramsey and Larry LeFleur for their useful contributions in developing these approaches

## Appendix 1

### Mathematical symbols used:

$\alpha$	probability of false positives.
$b$	slope of calibration curve.
$\beta$	probability of false negatives.
$g$	a "significance test" for the slope of the calibration line. equals $[(\text{RMSE})^2 \cdot (t_{n-2, 1-[\alpha/2]})] \div [(b^2) \cdot (S_{xx})]$ . should be less than 0.1 for each curve.

$n$	the number of observations in the calibration design.
$R(0)$	$R(z)$ where the concentration is zero (i.e., the blank).
$R(x_{D_{\text{est}}})$	$R(z)$ where the concentration is $x_{D_{\text{est}}}$ .
$R(z)$	$\{1 + 1/n + [(z - x_{\text{avg}})^2 / S_{xx}]\}^{1/2}$ .
$R^2_{\text{adj}}$	$R^2$ , "penalized" for each independent variable used in the regression. ( $R^2$ measures the amount of total variation in the response "explained" by the dependent variable.)
RMSE	root mean square error (often used for sample standard deviation).
$s$	sample standard deviation (often, RMSE is used).
$S_{xx}$	sum of squares, $\Sigma(x - x_{\text{avg}})^2$ .
$\sigma$	true standard deviation.
$t$	Student's $t$ for a specific $\alpha$ (or $\beta$ ) and specific degrees of freedom.
$x_{\text{avg}}$	average concentration (here in ppt).
$x_D$	a detection limit (here in ppt).
$x_{D_{\text{est}}}$	an estimated detection limit (here in ppt).
$z$	a concentration (here, in ppt).

### Terms used:

DL	detection limit. The concentration below which the analytical method cannot reliably detect a response.
H–V Level	Hubaux–Vos.
OLS	the concentration of a standard (includes blanks).
R.S.D.	ordinary least squares. A fitting technique that minimizes the sum of squares of the residuals.
Run	relative standard deviation (standard deviation divided by the mean).
Sequence	any series of standards prepared and analyzed all on one day. (Run numbers are given chronologically.)
Threshold, $T$	a set of Runs made in chronological order. For example, a Sequence of four would be Runs from days 1, 2, 3 and 4; or from days 5, 6, 7 and 8.
	the measurement response below which nothing can be detected reliably. The response cut-off between detection and non-detection.

**WLS**            weighted least squares. Same as OLS, except weights are added to account for non-constant response variation.

## References

- [1] Texas Instruments specification for deionized water.
- [2] USEPA, Appendix B to Part 136 —Definition and Procedure for the Determination of the Method Detection Limit—Revision 1.11, Federal Register 49 (209), 43430, October 26, 1984. Also referred to as “40 CFR Part 136”.
- [3] L.E. Vanatta, *J. Chromatogr.*, 739 (1996) 199.
- [4] A. Hubaux and G. Vos, *Anal. Chem.*, 42 (1970) 849.
- [5] R. Calcutt and R. Boddy, *Statistics for Analytical Chemists*, Chapman and Hall, New York, 1983.
- [6] D. Coleman, Technical memo, Alcoa Labs, March 26, 1993.
- [7] R. Gibbons, *Statistical Methods for Groundwater Monitoring*, Wiley, New York, 1994.
- [8] P.C. Meier and R.E. Zund, *Statistical Methods in Analytical Chemistry*, Wiley, New York, 1993.
- [9] R. Ferrus and M.R. Egea, *Anal. Chim. Acta*, 287 (1994) 119.
- [10] S.N. Ketkar, J.G. Dulak, S. Dheandhanoo and W.L. Fite, *Anal. Chim. Acta*, 245 (1991) 267.
- [11] M.F. Delaney, *Chemom. Intell. Lab. Syst.*, 3 (1988) 45.
- [12] R. Cassidy and M. Janosk, *LC–GC*, 10 (1992) 692.